RIGOROUS SOLUTION FOR AXIALLY-COMPRESSED CYLINDRICAL PANELS

Eliseu Lucena Neto

Francisco Alex Correia Monteiro

Paulo de Tarso Machado Leite Soares

eliseu@ita.br

facm@ita.br

paulotsoares@gmail.com

Instituto Tecnológico de Aeronáutica

Praça Marechal Eduardo Gomes, 50, 12228-900, São José dos Campos, SP, Brazil

Abstract. *An exact solution, based on Lévy method, is presented for the linear buckling of axially compressed circular cylindrical panels with stringers attached to the straight edges. The boundary conditions differ from the classical simply supported ones by taking into account the torsional and warping rigidities of the stringers. The reported exact buckling solutions may be valuable as benchmark data.*

Keywords: *Exact solution, Cylindrical panels, Buckling analysis*

1 INTRODUCTION

Circular cylindrical panels are important structural components in many engineering applications, such as aircraft fuselages, exteriors of rockets, submarine hulls, offshore platforms, and many others. The skin of a fuselage, for instance, can be thought of as an assembly of cylindrical panels supported by frames (circumferential stiffeners) and stringers (longitudinal stiffeners). Typically, these panels are the structural components most susceptible to buckling (Kollár & Dulácska, 1984, Buermann et al., 2006).

The classical simply supported conditions, often assumed for design purposes, are represented by the requirement that the radial displacements and the bending moments be zero along the edges of an isolated panel, in addition to the constraint of null tangential displacements and normal in-plane stress resultants associated to the buckling deformation. Unlike the above-mentioned conditions, in this work the bending moments along the panel straight edges are not made zero but equal to the torsion resisted by the attached stringers. This will make these edges to be somewhere between simply supported and clamped. The linearized Donnell's equations, with prebuckling rotations neglected, are chosen to describe the panel buckling behavior (Brush & Almroth, 1975).

The stringers are supposed to resist torsion in two ways: the first is denoted by Saint-Venant torsion, the second by warping torsion (Wunderlich & Pilkey, 2002). For most practical cases, one contribution may be neglected as compared to the other. Warping torsion is usually negligible in bars with solid or thin-walled closed cross sections. Saint-Venant torsion, on the other hand, may be neglected in thin-walled open cross sections (Kollbrunner & Basler, 1969). Our exact solution is independent of whether the Saint-Venant torsion or the warping torsion are resisted separately or together, and can be used to judge the relevance of each contribution if desired.

The exact solution for buckling of axially-compressed cylindrical panels with all edges simply supported is well-known (Timoshenko & Gere, 1961). Inclusion of the torsional resistance due to stringers attached to the straight edges makes the problem much more complicated. The exact solutions presented by Paik & Thayamballi (2000) and Bisagni & Vescovini (2009), for instance, are specifically for flat panels and neglect the warping torsion contribution. Recently, Soares (2015) has proposed an exact solution to the problem, as it is posed herein, based on a Lévy-type procedure where the effects of the panel aspect ratio, shallowness, stringer torsional resistance and the number of longitudinal buckle half-waves on the critical load are discussed.

2 BUCKLING PROBLEM

Figure 1a depicts a circular cylindrical panel of radius R, length a, width b and thickness h, subjected to a uniform distributed axial compressive force p per unit length and referred to a set of orthogonal curvilinear coordinates xyz placed in the panel midsurface. The panel buckling is supposed to be described by the linearized Donnell's equations

$$\nabla^4 u = -\frac{\nu}{R} w_{,xxx} + \frac{1}{R} w_{,xyy} \qquad \nabla^4 v = -\frac{2+\nu}{R} w_{,xxy} - \frac{1}{R} w_{,yyy}$$
$$D\nabla^8 w + \frac{Eh}{R^2} w_{,xxxx} + p\nabla^4 w_{,xx} = 0 \tag{1}$$

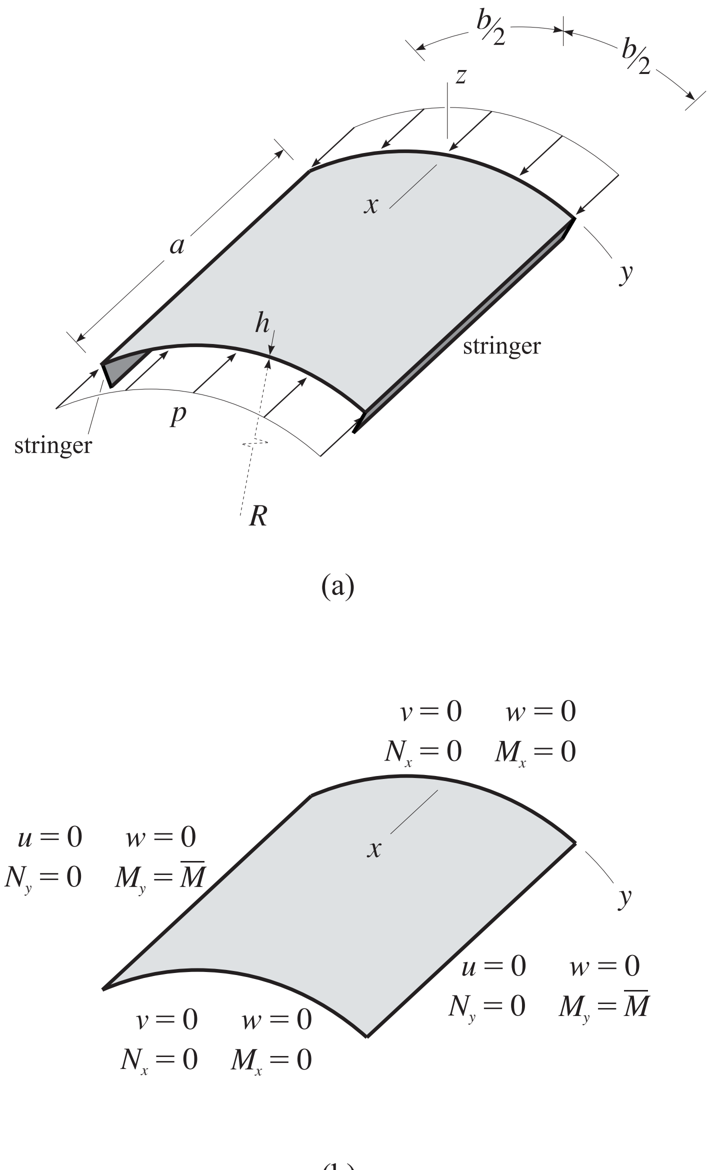

(a)

(b)

Figure 1: Cylindrical panel: (a) geometry and loading; (b) boundary conditions

with prebuckling rotations neglected (Brush & Almroth, 1975). The quantities u, v and w are the midsurface displacements in the x, y and z directions, E is the Young's modulus, ν is the Poisson's ratio, $D = Eh^3/12(1-\nu^2)$ defines the panel bending rigidity, ∇^8 denotes two sucessive applications of the two-dimensional biharmonic operator $\nabla^4(\ ) = (\ )_{,xxxx} + 2(\ )_{,xxyy} + (\ )_{,yyyy}$ and a comma followed by x (or y) indicates differentiation with respect to x (or y).

The boundary conditions (Figure 1b) to be applied differ from the classical simply supported ones in the sense that the torsion resisted by the stringers attached to the panel straight edges are also taken into account:

$$
\begin{array}{lllllll}
N_x = 0 & v = 0 & w = 0 & M_x = 0 & \text{at} & x = 0, a & \\
u = 0 & N_y = 0 & w = 0 & M_y = \bar{M} & \text{at} & y = \pm b/2. & (2)
\end{array}
$$

The in-plane forces N_x, N_y and the bending moments M_x, M_y are related to the midsurface displacements by means of

$$\begin{aligned} N_x &= \frac{Eh}{1-\nu^2}\left[u_{,x} + \nu\left(v_{,y} + \frac{w}{R}\right)\right] & N_y &= \frac{Eh}{1-\nu^2}\left(v_{,y} + \frac{w}{R} + \nu u_{,x}\right) \\ M_x &= -D\left(w_{,xx} + \nu w_{,yy}\right) & M_y &= -D\left(w_{,yy} + \nu w_{,xx}\right) \end{aligned} \tag{3}$$

and the external moments (Wunderlich & Pilkey, 2002)

$$\bar{M}(x, \pm b/2) = \mp G_s J_s w_{,xxy}(x, \pm b/2) \pm E_s \Gamma_s w_{,xxxxy}(x, \pm b/2) \tag{4}$$

exerted by the stringers on the panel edges $y = \pm b/2$ prevent them from rotating freely. The stringers have torsional and warping constants given by J_s and Γ_s, and material with Young's modulus E_s and shear modulus G_s. The first and second terms in $\bar{M}$ are associated to Saint-Venant and warping torsions, respectively.

An exact solution of Eq. (1) subjected to Eq. (2) can be accomplished most conveniently by introducing the nondimentional coordinates

$$\xi = \sqrt{\frac{2Eh}{p_{cl}}}\frac{x}{R} \qquad \eta = \sqrt{\frac{2Eh}{p_{cl}}}\frac{y}{R} \tag{5}$$

suggested by Nachbar (1962), where

$$p_{cl} = \frac{Eh^2}{R\sqrt{3\left(1-\nu^2\right)}}. \tag{6}$$

The classical value p_{cl} identifies the minimum buckling load that a simply supported panel could ever achieved (Timoshenko & Gere, 1961), according to the adopted linear buckling analysis. Referred to these new coordinates, the system of equations Eq. (1) becomes

$$\begin{aligned} &\nabla^4 u = -\nu w_{,\xi\xi\xi} + w_{,\xi\eta\eta} \qquad \nabla^4 v = -\left(2+\nu\right) w_{,\xi\xi\eta} - w_{,\eta\eta\eta} \\ &\nabla^8 w + w_{,\xi\xi\xi\xi} + 2\rho\nabla^4 w_{,\xi\xi} = 0 \end{aligned} \tag{7}$$

while the set of boundary conditions Eq. (2) writes

$$\begin{aligned} N_\xi &= 0 & v &= 0 & w &= 0 & M_\xi &= 0 & &\text{at} & \xi &= 0, \xi_0 \\ u &= 0 & N_\eta &= 0 & w &= 0 & M_\eta &= \bar{M} & &\text{at} & \eta &= \pm\eta_0 \end{aligned} \tag{8}$$

with

$$\rho = \frac{p}{p_{cl}} \qquad \xi_0 = \sqrt{\frac{2Eh}{p_{cl}}}\frac{a}{R} \qquad \eta_0 = \sqrt{\frac{2Eh}{p_{cl}}}\frac{b}{2R}. \tag{9}$$

In Eqs. (7) and (8), the operators ∇^4 and ∇^8 are written in the new coordinates ξ and η. The quantities

$$u\left(\xi,\eta\right) = \sqrt{\frac{2Eh}{p_{cl}}}\frac{u\left(x,y\right)}{R} \qquad v\left(\xi,\eta\right) = \sqrt{\frac{2Eh}{p_{cl}}}\frac{v\left(x,y\right)}{R} \qquad w\left(\xi,\eta\right) = \frac{w\left(x,y\right)}{R} \tag{10}$$

now represent nondimensional displacement parameters and

$$N_\xi = \frac{Eh}{1-\nu^2}\left(u_{,\xi} + \nu v_{,\eta} + \nu w\right) \qquad N_\eta = \frac{Eh}{1-\nu^2}\left(\nu u_{,\xi} + v_{,\eta} + w\right)$$
$$M_\xi = -\frac{D}{R}\frac{2Eh}{p_{cl}}\left(w_{,\xi\xi} + \nu w_{,\eta\eta}\right) \qquad M_\eta = -\frac{D}{R}\frac{2Eh}{p_{cl}}\left(\nu w_{,\xi\xi} + w_{,\eta\eta}\right)$$
$$\bar{M}\left(\xi, \pm\eta_0\right) = \mp\frac{G_s J_s}{R^2}\left(\frac{2Eh}{p_{cl}}\right)^{3/2} w_{,\xi\xi\eta}\left(\xi, \pm\eta_0\right) \pm \frac{E_s \Gamma_s}{R^4}\left(\frac{2Eh}{p_{cl}}\right)^{5/2} w_{,\xi\xi\xi\xi\eta}\left(\xi, \pm\eta_0\right). \tag{11}$$

A general buckling mode satisfying the simply supported boundary conditions on edges $\xi = 0$, ξ_0 can be assumed in the form

$$u(\xi,\eta) = U(\eta)\cos k\xi \qquad v(\xi,\eta) = V(\eta)\sin k\xi \qquad w(\xi,\eta) = W(\eta)\sin k\xi, \tag{12}$$

with

$$k = \frac{m\pi R}{a}\sqrt{\frac{p_{cl}}{2Eh}} \tag{13}$$

and the integer m standing for the number of half-waves in the longitudinal direction. The functions $U(\eta)$, $V(\eta)$ and $W(\eta)$ must be obtained so that the mode fulfills the conditions required by the supports at $\eta = \pm\eta_0$ and satisfies Eq. (7).

After substitution of Eq. (12), the boundary conditions Eq. (8) on edges $\eta = \pm\eta_0$ hold for every $0 < \xi < \xi_0$ if

$$U(\pm\eta_0) = 0 \qquad W(\pm\eta_0) = 0 \qquad V_{,\xi}(\pm\eta_0) = 0$$
$$\frac{D}{R}W_{,\xi\xi}(\pm\eta_0) \pm \left(G_s J_s + E_s\Gamma_s \frac{2Eh}{p_{cl}}\frac{k^2}{R^2}\right)\left(\frac{2Eh}{p_{cl}}\right)^{1/2}\frac{k^2}{R^2}W_{,\xi}(\pm\eta_0) = 0. \tag{14}$$

On the other hand, the equation obtained after substitution of $w(\xi,\eta)$ into the third of equations Eq. (7) holds for every point (ξ,η) of the domain for nontrivial w (i.e., $W \neq 0$) if

$$\frac{d^8W}{d\eta^8} - 4k^2\frac{d^6W}{d\eta^6} + 2k^2\left(3k^2 - \rho\right)\frac{d^4W}{d\eta^4} - 4k^4\left(k^2 - \rho\right)\frac{d^2W}{d\eta^2} + k^4\left(k^4 - 2k^2\rho + 1\right)W = 0. \tag{15}$$

Particular solutions of this homogeneous linear differential equation are in the form e^{sx}, where s denotes a root of the algebraic equation

$$s^8 - 4k^2 s^6 + 2k^2\left(3k^2 - \rho\right)s^4 - 4k^4\left(k^2 - \rho\right)s^2 + k^4\left(k^4 - 2k^2\rho + 1\right) = 0. \tag{16}$$

The roots of Eq. (16) can be easily found by rewriting the equation as

$$\left(s^2 - k^2\right)^4 - 2\rho k^2\left(s^2 - k^2\right)^2 + k^4 = 0 \tag{17}$$

from which

$$s = \pm\sqrt{k^2 \pm k\sqrt{\rho \pm \sqrt{\rho^2 - 1}}}. \tag{18}$$

Let the eight roots be defined as

$$s_1 = -s_5 = \sqrt{k^2 - k\sqrt{\rho - \sqrt{\rho^2 - 1}}} \qquad s_2 = -s_6 = \sqrt{k^2 - k\sqrt{\rho + \sqrt{\rho^2 - 1}}}$$
$$s_3 = -s_7 = \sqrt{k^2 + k\sqrt{\rho - \sqrt{\rho^2 - 1}}} \qquad s_4 = -s_8 = \sqrt{k^2 + k\sqrt{\rho + \sqrt{\rho^2 - 1}}}. \quad (19)$$

For the numerical analysis, it is convenient to identify whether the roots are real or complex, and equal or distinct.

It is clear from physical considerations that the buckling will always take place for $\rho > 1$ due to the attachment of stringers to the panel edges $\eta = \pm\eta_0$. This constraint makes

$$\rho \pm \sqrt{\rho^2 - 1} > 0. \quad (20)$$

As the parameter $k > 0$, the roots s_3, s_4, s_7, s_8 are real and distinct, and now rewritten as

$$s_3 = -s_7 = \alpha_3 \qquad s_4 = -s_8 = \alpha_4$$
$$\alpha_3 = \sqrt{k^2 + k\sqrt{\rho - \sqrt{\rho^2 - 1}}} \qquad \alpha_4 = \sqrt{k^2 + k\sqrt{\rho + \sqrt{\rho^2 - 1}}}. \quad (21)$$

On the other hand, the remaining roots s_1, s_2, s_5, s_6 may be real or purely imaginary, depending on the values of ρ and k, and grouped according to the five cases in the sequel.

Case I: $0 < k^2 < \rho - \sqrt{\rho^2 - 1}$

The roots s_1, s_2, s_5, s_6 are purely imaginary:

$$s_1 = -s_5 = i\beta_1 \qquad s_2 = -s_6 = i\beta_2$$
$$\beta_1 = \sqrt{k\sqrt{\rho - \sqrt{\rho^2 - 1}} - k^2} \qquad \beta_2 = \sqrt{k\sqrt{\rho + \sqrt{\rho^2 - 1}} - k^2} \quad (22)$$

with the imaginary unit denoted by $i = \sqrt{-1}$. The solution of Eq. (15) may then be taken in the form

$$W(\eta) = W_1 \sin\beta_1\eta + W_2 \cos\beta_1\eta + W_3 \sin\beta_2\eta + W_4 \cos\beta_2\eta$$
$$+ W_5 \sinh\alpha_3\eta + W_6 \cosh\alpha_3\eta + W_7 \sinh\alpha_4\eta + W_8 \cosh\alpha_4\eta \quad (23)$$

where W_i are arbitrary constants.

Because the xz plane is a symmetry plane for the problem (Figure 1a), the buckling modes can be separated into two distinct symmetry classes, which may be readily identified by the shape of $W(\eta)$. The modes may be classified by whether the displacement component w is symmetric or antisymmetric with respect to the xz plane. The displacement components u and v will then also have appropriate symmetries. This separation not only aids in identifying and classifying the buckling mode, but also reduces the eigenvalue problem to two distinct problems with smaller determinants to be evaluated. Using the subscripts "s" and "a" to refer to symmetric and antisymmetric modes, Eq. (23) is splitted into

$$W_s(\eta) = W_{1s} \cos\beta_1\eta + W_{2s} \cos\beta_2\eta + W_{3s} \cosh\alpha_3\eta + W_{4s} \cosh\alpha_4\eta$$
$$W_a(\eta) = W_{1a} \sin\beta_1\eta + W_{2a} \sin\beta_2\eta + W_{3a} \sinh\alpha_3\eta + W_{4a} \sinh\alpha_4\eta \quad (24)$$

where W_{is} and W_{ia} are appropriate redefinitions of W_i. From Eqs. (7), (12) and (24), the functions $U(\eta)$ and $V(\eta)$ may also be splitted into

$$\begin{aligned}
U_s(\eta) &= U_{1s}\cos\beta_1\eta + U_{2s}\cos\beta_2\eta + U_{3s}\cosh\alpha_3\eta + U_{4s}\cosh\alpha_4\eta \\
U_a(\eta) &= U_{1a}\sin\beta_1\eta + U_{2a}\sin\beta_2\eta + U_{3a}\sinh\alpha_3\eta + U_{4a}\sinh\alpha_4\eta \\
V_s(\eta) &= V_{1s}\sin\beta_1\eta + V_{2s}\sin\beta_2\eta + V_{3s}\sinh\alpha_3\eta + V_{4s}\sinh\alpha_4\eta \\
V_a(\eta) &= V_{1a}\cos\beta_1\eta + V_{2a}\cos\beta_2\eta + V_{3a}\cosh\alpha_3\eta + V_{4a}\cosh\alpha_4\eta
\end{aligned} \tag{25}$$

with

$$U_{is} = u_{is}W_{is} \qquad U_{ia} = u_{ia}W_{ia} \qquad V_{is} = v_{is}W_{is} \qquad V_{ia} = v_{ia}W_{ia}. \tag{26}$$

The quantities u_{is}, u_{ia}, v_{is} and v_{ia} are detailed in Soares (2015).

Introduction of the symmetric (or antisymmetric) displacement components Eqs. (24) and (25) into Eq. (14) yields the homogeneous system of equations

$$[K]\{W\} = \{0\}, \tag{27}$$

where $\{W\}$ collects W_{is} (or W_{ia}) and matrix $[K]$ is given in Soares (2015). Each root ρ of the equation $\det[K] = 0$ represents a buckling load. Similar expressions to Eqs. (26) and (27) hold for the remaining cases, for which the quantities u_{is}, u_{ia}, v_{is}, v_{ia} and matrix $[K]$ are also given in Soares (2015), and only the displacement components will be then summarized next.

Case II: $k^2 = \rho - \sqrt{\rho^2 - 1}$

The roots s_1, s_5 are null and s_2, s_6 are purely imaginary:

$$s_1 = s_5 = 0 \qquad s_2 = -s_6 = i\beta_2. \tag{28}$$

Splitting the solution of Eq. (15) into symmetric and antisymetric modes, as done in Case I,

$$\begin{aligned}
W_s(\eta) &= W_{1s} + W_{2s}\cos\beta_2\eta + W_{3s}\cosh\alpha_3\eta + W_{4s}\cosh\alpha_4\eta \\
W_a(\eta) &= W_{1a}\eta + W_{2a}\sin\beta_2\eta + W_{3a}\sinh\alpha_3\eta + W_{4a}\sinh\alpha_4\eta \\
U_s(\eta) &= U_{1s} + U_{2s}\cos\beta_2\eta + U_{3s}\cosh\alpha_3\eta + U_{4s}\cosh\alpha_4\eta \\
U_a(\eta) &= U_{1a}\eta + U_{2a}\sin\beta_2\eta + U_{3a}\sinh\alpha_3\eta + U_{4a}\sinh\alpha_4\eta \\
V_s(\eta) &= V_{2s}\sin\beta_2\eta + V_{3s}\sinh\alpha_3\eta + V_{4s}\sinh\alpha_4\eta \\
V_a(\eta) &= V_{1a} + V_{2a}\cos\beta_2\eta + V_{3a}\cosh\alpha_3\eta + V_{4a}\cosh\alpha_4\eta.
\end{aligned} \tag{29}$$

Case III: $\rho - \sqrt{\rho^2 - 1} < k^2 < \rho + \sqrt{\rho^2 - 1}$

The roots s_1, s_5 are real and s_2, s_6 are purely imaginary:

$$s_1 = -s_5 = \alpha_1 \qquad s_2 = -s_6 = i\beta_2 \qquad \alpha_1 = \sqrt{k^2 - k\sqrt{\rho - \sqrt{\rho^2 - 1}}}. \tag{30}$$

The solution of Eq. (15) in this case is

$$\begin{aligned}
W_s(\eta) &= W_{1s}\cosh\alpha_1\eta + W_{2s}\cos\beta_2\eta + W_{3s}\cosh\alpha_3\eta + W_{4s}\cosh\alpha_4\eta \\
W_a(\eta) &= W_{1a}\sinh\alpha_1\eta + W_{2a}\sin\beta_2\eta + W_{3a}\sinh\alpha_3\eta + W_{4a}\sinh\alpha_4\eta \\
U_s(\eta) &= U_{1s}\cosh\alpha_1\eta + U_{2s}\cos\beta_2\eta + U_{3s}\cosh\alpha_3\eta + U_{4s}\cosh\alpha_4\eta \\
U_a(\eta) &= U_{1a}\sinh\alpha_1\eta + U_{2a}\sin\beta_2\eta + U_{3a}\sinh\alpha_3\eta + U_{4a}\sinh\alpha_4\eta \\
V_s(\eta) &= V_{1s}\sinh\alpha_1\eta + V_{2s}\sin\beta_2\eta + V_{3s}\sinh\alpha_3\eta + V_{4s}\sinh\alpha_4\eta \\
V_a(\eta) &= V_{1a}\cosh\alpha_1\eta + V_{2a}\cos\beta_2\eta + V_{3a}\cosh\alpha_3\eta + V_{4a}\cosh\alpha_4\eta.
\end{aligned} \tag{31}$$

Case IV: $k^2 = \rho + \sqrt{\rho^2 - 1}$

The roots s_1, s_5 are real and s_2, s_6 are null:

$$s_1 = -s_5 = \alpha_1 \qquad s_2 = s_6 = 0. \tag{32}$$

Now, the solution of Eq. (15) is

$$\begin{aligned}
W_s(\eta) &= W_{1s}\cosh\alpha_1\eta + W_{2s} + W_{3s}\cosh\alpha_3\eta + W_{4s}\cosh\alpha_4\eta \\
W_a(\eta) &= W_{1a}\sinh\alpha_1\eta + W_{2a}\eta + W_{3a}\sinh\alpha_3\eta + W_{4a}\sinh\alpha_4\eta \\
U_s(\eta) &= U_{1s}\cosh\alpha_1\eta + U_{2s} + U_{3s}\cosh\alpha_3\eta + U_{4s}\cosh\alpha_4\eta \\
U_a(\eta) &= U_{1a}\sinh\alpha_1\eta + U_{2a}\eta + U_{3a}\sinh\alpha_3\eta + U_{4a}\sinh\alpha_4\eta \\
V_s(\eta) &= V_{1s}\sinh\alpha_1\eta + V_{3s}\sinh\alpha_3\eta + V_{4s}\sinh\alpha_4\eta \\
V_a(\eta) &= V_{1a}\cosh\alpha_1\eta + V_{2a} + V_{3a}\cosh\alpha_3\eta + V_{4a}\cosh\alpha_4\eta.
\end{aligned} \tag{33}$$

Case V: $k^2 > \rho + \sqrt{\rho^2 - 1}$

The roots s_1, s_2, s_5, s_6 are all real:

$$s_1 = -s_5 = \alpha_1 \qquad s_2 = -s_6 = \alpha_2 \qquad \alpha_2 = \sqrt{k^2 - k\sqrt{\rho + \sqrt{\rho^2 - 1}}}. \tag{34}$$

The solution of Eq. (15) reduces to

$$\begin{aligned}
W_s(\eta) &= W_1\cosh\alpha_1\eta + W_2\cosh\alpha_2\eta + W_3\cosh\alpha_3\eta + W_4\cosh\alpha_4\eta \\
W_a(\eta) &= W_1\sinh\alpha_1\eta + W_2\sinh\alpha_2\eta + W_3\sinh\alpha_3\eta + W_4\sinh\alpha_4\eta \\
U_s(\eta) &= U_1\cosh\alpha_1\eta + U_2\cosh\alpha_2\eta + U_3\cosh\alpha_3\eta + U_4\cosh\alpha_4\eta \\
U_a(\eta) &= U_1\sinh\alpha_1\eta + U_2\sinh\alpha_2\eta + U_3\sinh\alpha_3\eta + U_4\sinh\alpha_4\eta \\
V_s(\eta) &= V_1\sinh\alpha_1\eta + V_2\sinh\alpha_2\eta + V_3\sinh\alpha_3\eta + V_4\sinh\alpha_4\eta \\
V_a(\eta) &= V_1\cosh\alpha_1\eta + V_2\cosh\alpha_2\eta + V_3\cosh\alpha_3\eta + V_4\cosh\alpha_4\eta.
\end{aligned} \tag{35}$$

NUMERICAL RESULTS

The eigenvalue problem Eq. (27) cannot be written in a form to allow the direct use of some standard software package to solve it. The following iteration steps is then employed to identify the smallest root ρ of $\det[K] = 0$ for a given m:

1. evaluate k from Eq. (13);

2. define the open intervals $I_1 = (1, \alpha)$ and $I_2 = (\alpha, 2\alpha)$ with $\alpha = (k^4 + 1)/2k^2$;

3. state the small increment $\Delta I_1 = (\alpha - 1)/10000$ and $\Delta I_2 = \alpha/10000$;

4. if $k < 1$ then Case I, II or III applies.

   Case I: starting from $\rho = 1 + \Delta I_1$, verify the sign of $\det[K]$ with k_{ij} given for symmetric and for antisymmetric modes. Increase progressively the value of ρ by increments ΔI_1 until either the determinant sign changes or ρ reaches α. If the determinant sign changes, there is a root in the subinterval $I = [\rho - \Delta I_1, \rho]$ and go to step 7. If ρ reaches α, then there is no roots in I_1 and go to Case II.

   Case II: setting $\rho = \alpha$, verify if $\det[K] = 0$ with k_{ij} given for symmetric and for antisymmetric modes. If yes, save the root $\rho = \alpha$ and go to step 8. Otherwise, go to Case III. It has been accepted as null the value $|\det[K]| < 10^{-9}$.

   Case III: starting from $\rho = \alpha + \Delta I_2$, verify the sign of $\det[K]$ with k_{ij} given for symmetric and for antisymmetric modes. Increase progressively the value of ρ by increments ΔI_2 until either the determinant sign changes or ρ reaches 2α. If the determinant sign changes, there is a root in the subinterval $I = [\rho - \Delta I_2, \rho]$ and go to step 7. If ρ reaches 2α, then there is no roots in I_2 and stop the search for the given m;

5. if $k = 1$ then only Case III applies. Do the Case III process as described above;

6. if $k > 1$ then Case V, IV or III applies.

   Case V: starting from $\rho = 1 + \Delta I_1$, verify the sign of $\det[K]$ with k_{ij} given for symmetric and for antisymmetric modes. Do the same process as described for Case I. If ρ reaches α, then there is no roots in I_1 and go to Case IV.

   Case IV: setting $\rho = \alpha$, verify if $\det[K] = 0$ with k_{ij} given for symmetric and for antisymmetric modes. If yes, save the root $\rho = \alpha$ and go to step 8. Otherwise, do the Case III process as described above. It has been accepted as null the value $|\det[K]| < 10^{-9}$;

7. search for the root in the subinterval using some iterative methods. Herein we have employed the *fzero* function of MATLAB that finds a point where the function changes sign using a combination of bisection, secant, and inverse quadratic interpolation methods. Save the root;

8. retain the smallest root ρ, for the given m, with regard to the symmetric and antisymmetric modes.

The critical value of ρ corresponds to the smallest value identified for $m = 1, 2, 3, \ldots$

All the analyzed panels have length $a = 500$ mm, thickness $h = 1$ mm, and material defined by $E = 72400$ N/mm^2, $\nu = 0.33$. Several values are attributed to the width b, radius R, and also to the stringer parameters J_s and Γ_s. The stringer material is given by $E_s = 71020$ N/mm^2, $G_s = 26700$ N/mm^2.

Table 1 summarizes the effect of the aspect ratio b/a and radius-to-thickness ratio R/h on the critical value of ρ for panels under different stringer torsional J_s and warping Γ_s constants. The half-wave number (m), mode type (symmetric, antisymmetric), and solution case (I, II, III, IV, V) are indicated in parentheses. Pairs ($J_s \neq 0$, $\Gamma_s \neq 0$) identify panels with stringers attached to the straight edges. For such panels, the exact buckling loads presented in Table 1 may be considerably higher than those predicted by neglecting the stringer contribution. With ($J_s = 0$, $\Gamma_s = 0$), the buckling load is underpredicted mainly for narrower (small b/a) and shallower (large R/h) panels. For instance, a panel with $b/a = 0.2$ and $R/h = 1500$ attached to stringers with ($J_s = 96$ mm^4, $\Gamma_s = 36370$ mm^6) buckles at a load somewhat 51% higher than that load obtained by neglecting the stringer contribution.

Table 1: Effect of the aspect ratio b/a and radius-to-thickness ratio R/h on the critical value of ρ for panels under several pairs (J_s, Γ_s) of stringer constants

		R/h		
(J_s, Γ_s)	b/a	500	1000	1500
(96, 36370)	0.2	1.08832 (11, s, III)	1.37401 (8, s, III)	1.78693 (8, s, III)
	0.4	1.00728 (12, s, I)	1.02491 (8, s, I)	1.05119 (7, s, III)
	0.6	1.00280 (13, s, III)	1.00579 (9, s, III)	1.00995 (7, s, III)
	0.8	1.00125 (13, s, III)	1.00178 (9, s, III)	1.00481 (7, s, I)
	1.0	1.00074 (13, s, III)	1.00071 (9, s, III)	1.00427 (7, s, I)
	1.2	1.00052 (13, s, III)	1.00036 (9, s, III)	1.00360 (7, a, I)
	1.4	1.00041 (13, s, III)	1.00023 (9, s, I)	1.00246 (7, a, I)
(12372, 1582)	0.2	1.08939 (11, s, III)	1.38442 (8, s, III)	1.80290 (8, s, III)
	0.4	1.00731 (12, s, I)	1.02539 (8, s, I)	1.05271 (7, s, III)
	0.6	1.00281 (13, s, III)	1.00585 (9, s, III)	1.01021 (7, s, III)
	0.8	1.00125 (13, s, III)	1.00180 (9, s, III)	1.00487 (7, s, I)
	1.0	1.00074 (13, s, III)	1.00072 (9, s, III)	1.00428 (7, s, I)
	1.2	1.00052 (13, s, III)	1.00036 (9, s, III)	1.00367 (7, a, I)
	1.4	1.00041 (13, s, III)	1.00023 (9, s, I)	1.00248 (7, a, I)

3 CONCLUSIONS

A Lévy-type procedure is adopted to develop, in a suitable detail, an exact solution for buckling of axially-compressed cylindrical panels with stringers attached to the straight edges. The linearized Donnell's equations, with prebuckling rotations neglected, are chosen to describe the buckling behavior. Both Saint-Venant and warping torsions resisted by the stringers are taken into account. For convenience, rather than a necessity, the solution is restricted to load parameters $\rho > 1$ by anticipating the stringer presence. An algorithm to generate numerical results is provided. Sets of exact results for specific panels and stringers are tabled with which those from approximated procedures may be directly compared. The attached stringers have a noteworthy influence on the buckling load for narrower (small b/a) and shallower (large R/h) panels.

REFERENCES

Bisagni, C., & Vescovini, R., 2009. Analytical formulation for local buckling and post-buckling analysis of stiffened laminated panels. *Thin-Walled Structures*, vol. 47, n. 3, pp. 318-334.

Brush, D. O., & Almroth, B. O., 1975. *Buckling of Bars, Plates, and Shells*. McGraw-Hill.

Buermann, P., Rolfes, R., Tessmer, J., & Schagerl, M., 2006. A semi-analytical model for local post-buckling analysis of stringer- and frame-stiffened cylindrical panels. *Thin-Walled Structures*, vol. 44, n. 1, pp. 102-114.

Kollár, L., & Dulácska, E., 1984. *Buckling of Shells for Engineers*. Wiley.

Kollbrunner, C. F., & Basler, K., 1969. *Torsion in Structures*. Springer.

Nachbar, W., 1962. Characteristic roots for Donnell's equations with uniform axial prestress. *Journal of Applied Mechanics*, vol. 29, n. 2, pp. 434-435.

Paik, J. K., & Thayamballi, A. K., 2000. Buckling strength of steel plating with elastically restrained edges. *Thin-Walled Structures*, vol. 37, n. 1, pp. 27-55.

Reddy, J. N., 2004. *Mechanics of Laminated Composite Plates and Shells: Theory and Analysis*. 2nd edn. CRC Press.

Soares, P. T. M. L., 2015. *Flambagem de Painéis Cilíndricos sob Compressão Axial com as Bordas Retas Parcialmente Restritas à Rotação*. Tese de Mestrado, ITA/São José dos Campos.

Timoshenko, S. P., & Gere, J. M., 1961. *Theory of Elastic Stability*. 2nd edn. McGraw-Hill.

Wunderlich, W., & Pilkey, W. D., 2002. *Mechanics of Structures: Variational and Computational Methods*. 2nd edn. CRC Press.